Water-based synthesis and nitrate release properties of a Zr^{IV}-based metal-organic framework derived from *L*-aspartic acid

Temitope Olabisi Abodunrin,[a,b] Matouš Kloda,[c] Jan Demel[c] and Marco Taddei[b,d]*

Received 00th January 20xx,
Accepted 00th January 20xx

DOI: 10.1039/x0xx00000x

We report the synthesis and characterisation of a cationic metal-organic framework (MOF) based on Zr^{IV} and *L*-aspartate and containing nitrate as extraframework counteranion, named MIP-202-NO_3. The ion exchange properties of MIP-202-NO_3 were preliminarily investigated to evaluate its potential as a platform for controlled release of nitrate, finding that it readily releases nitrate in aqueous solution.

Nitrogen is an essential nutrient that is critical for increased crop productivity and is usually sourced through the application of nitrogenous fertilisers, such as urea, ammonium nitrate, liquid nitrogen fertiliser or complex fertilisers.[1,2] The use of fertilisers is responsible for about 50% of nitrogen-containing pollutants found in the environment, through volatilisation of ammonia, leaching of nitrates and by-products of nitrification/denitrification.[3] Nitrate is the second major cause of ground and surface water pollution after pesticides.[2] Nitrate pollution in water is due to the excessive or inadequate use of nitrogen fertilisers, discharge from sewage systems and animal wastes. The nitrate anion is only weakly adsorbed on soil particles and therefore it is easily dissolved in drainage water.[3] Nitrate has adverse effects on human and animal health and contributes to climate change by decomposing to nitrous oxide, a potent greenhouse gas.[2,4,5] Systems that allow a continuous and controlled release of nitrogen fertilisers are actively sought after to reduce the environmental impact of agricultural activities while ensuring high crop production levels.[1] Hydrogel formulations, ethylcellulose-coated granules of ammonium nitrate and nitrate-intercalated layered double hydroxides (LDHs) are among the solutions proposed in the literature for controlled release of nitrate fertilisers.[6–11]

The use of metal-organic frameworks (MOFs) in agriculture is attracting growing interest.[12–14] The porous nature of MOFs makes them suitable for use as host platforms for controlled release of both nutrients and pesticides,[15–19] as well as for their removal from the environment *via* either adsorption or degradation.[20–23] The ideal MOF to be used for such applications should be "green", that is, based on environmentally friendly metal and organic linker, and prepared in a non-toxic solvent, the most desirable being water. The stability of a MOF matrix intended for controlled release of fertilisers should be sufficient to guarantee the release of the nutrient over a convenient timeframe, but the matrix should ultimately be biodegraded to non-harmful by-products by environmental agents. To the best of our knowledge, there are no reports of MOFs evaluated as platforms for controlled release of nitrate to date.

Zr^{IV}-based MOFs have been proposed in the literature as potential drug delivery systems, owing to the biocompatibility and low toxicity of zirconium to either humans or plants.[24–26] Zr displays limited mobility and phytoavailability in the soil. After plant uptake, Zr mainly accumulates in root cells and a limited amount is translocated to plant shoots.[26] Herein, we report the water-based synthesis of a cationic Zr^{IV}-based MOF containing the naturally occurring α-amino acid *L*-aspartic acid (H_2Asp) as the linker and nitrate as an extra-framework anion. The chloride form of this MOF was first reported in 2018 by Wang *et al.* and named MIP-202 (Figure 1).[27] To evaluate the suitability of the nitrate form of MIP-202 (hereafter MIP-202-NO_3) as a platform for controlled release of nitrate, we have investigated its anion exchange properties in aqueous environment.

MIP-202-NO_3 was prepared using a water-based procedure (see ESI for further details), starting from zirconium oxynitrate tetrahydrate and H_2Asp, and adding concentrated HNO_3 to the

[a] *Department of Physical Sciences, College of Pure and Applied Sciences, Landmark University, P.M.B. 1001, Omu-aran, Kwara State, Nigeria*
[b] *Dipartimento di Chimica e Chimica Industriale, Unità di Ricerca INSTM, Università di Pisa, Via Giuseppe Moruzzi 13, 56124 Pisa, Italy. Email: marco.taddei@unipi.it*
[c] *Institute of Inorganic Chemistry of the Czech Academy of Sciences, Husinec-Řež-1001, 250 68 Řež, Czech Republic*
[d] *Centro per l'Integrazione della Strumentazione Scientifica dell'Università di Pisa (CISUP), Pisa, Italy*

† Footnotes relating to the title and/or authors should appear here.
Electronic Supplementary Information (ESI) available: [Synthetic procedures, SEM images, NMR spectra, PXRD patterns, ATR-IR spectra, CHN analysis, ICP-OES analysis, solvent stability experiments]. See DOI: 10.1039/x0xx00000x

reaction mixture. The presence of HNO_3 ensures that the reaction is conducted in strongly acidic environment that allows protonation of all the amino groups, leading to a crystalline product. Reactions carried out without HNO_3 fail to afford a solid under otherwise identical experimental conditions. MIP-202-Cl was synthesised by following the existing literature method,[27] increasing the time to 24 h to maximise the yield. The synthesis of MIP-202-Cl proceeds without the addition of a strong acid, thanks to the highly acidic environment produced by the release of two equivalents of HCl upon hydrolysis of $ZrCl_4$.

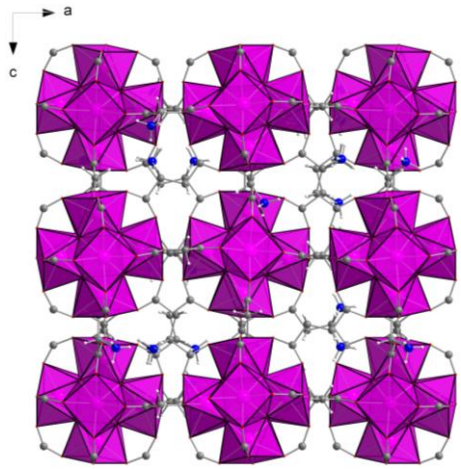

Figure 1. Crystal structure of MIP-202. Colour code: Zr, pink; C, grey; N, blue; O, red; H, white.

The powder X-ray diffraction (PXRD) pattern of MIP-202-NO_3 matches with that of MIP-202-Cl, confirming that the desired crystalline phase with face-centred cubic topology was successfully obtained (Figure 2a). The broader reflections in the pattern of MIP-202-NO_3 suggest that its crystallites are smaller than those of MIP-202-Cl. Scanning electron microscopy (SEM) micrographs confirm that MIP-202-NO_3 crystallites have in fact size below 100 nm and an ill-defined morphology (Figure S2). The attenuated total reflectance infrared (ATR-IR) spectra for MIP 202-NO_3 and MIP 202-Cl display similar bands, most notably the coordinated carboxylate stretching vibrations at 1613 cm^{-1} (asymmetric) and 1424 cm^{-1} (symmetric). Both MOFs contain large amounts of hydrogen-bonded water, as indicated by the broad O-H stretching band between 2750 and 3750 cm^{-1}. The small band at 1722 cm^{-1} in the spectrum of MIP-202-NO_3 is due to the presence of traces of acetone in this particular sample, which was washed once with acetone at the end of the workup procedure. The major difference, though, is represented by the intense band at 1320 cm^{-1} in the spectrum of MIP 202-NO_3, characteristic of the nitrate anion (Figure 2b).[28]

Based on CHN elemental analysis and quantitative ^1H and ^{35}Cl nuclear magnetic resonance (NMR) analysis performed on desolvated samples digested in 1 M NaOH (Figures S3-S5, Table S1), the chemical formulas for MIP-202-NO_3 and MIP-202-Cl are proposed to be $Zr_6O_4(OH)_4(Asp)_6(HNO_3)_6$ and $Zr_6O_4(OH)_4(Asp)_6(HCl)_{7.4}$, respectively. The excess of chloride found in MIP-202-Cl is consistent with previous observations.[27] The loading of nitrate in MIP-202-NO_3 is 20.3 wt% (determined on a dry basis), slightly lower than that of a $Mg_2Al(OH)_6(NO_3)$ LDH (25.8 wt%, determined on a dry basis). Thermogravimetric analysis (TGA) performed in oxidative atmosphere reveals a lower thermal stability for MIP-202-NO_3, whose framework starts degrading already below 200 °C, soon after desorption of water from the pores, than for MIP-202-Cl, whose degradation begins above 200 °C (Figure S6). MIP-202-NO_3 also contains a lower amount of solvent (12.4%) than MIP-202-Cl (24.9%), suggesting that the former is less porous, as can be expected based on the larger size and mass of the nitrate ion than the chloride ion. This is corroborated by the results of N_2 sorption analysis at 77 K, which reveals an isotherm with a shape indicative of a very small micropore volume (Figure S7).

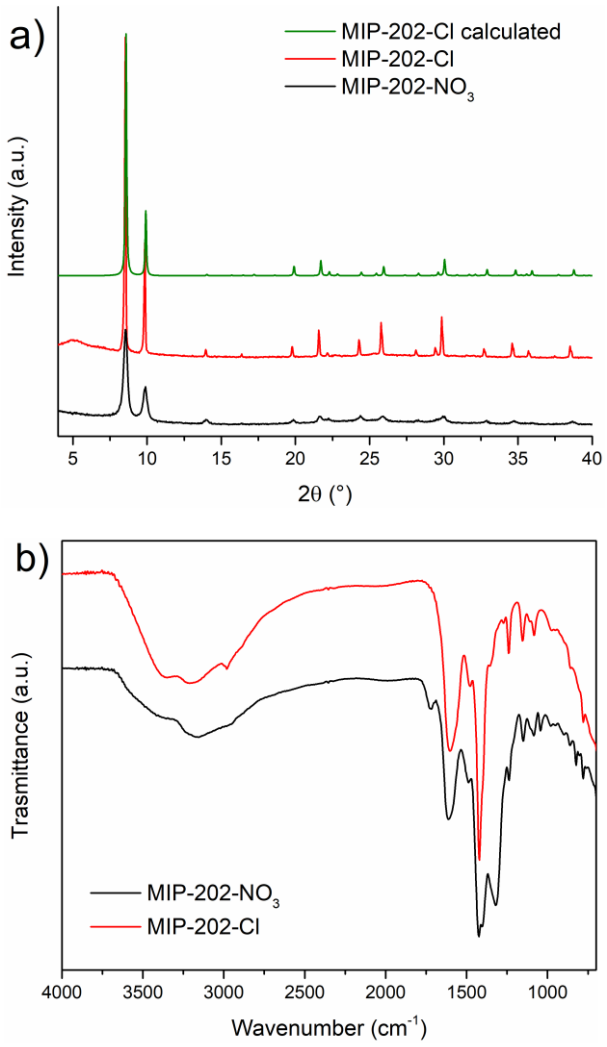

Figure 2. Comparison between the PXRD patterns (a) and ATR-IR spectra (b) of MIP-202-NO_3 (black) and MIP-202-Cl (red). The green pattern in Figure 2a was calculated from the crystallographic information file (CCDC deposition number 1842337).

The possibility to convert the two different forms of MIP-202 into each other by ion exchange was explored by soaking MIP-202-NO_3 in HCl 0.1 M and NaCl 0.1 M, and MIP-202-Cl in HNO_3 0.1 M and $NaNO_3$ 0.1 M. Soaking in acidic solutions led to recover powders with crystallinity comparable to that of the as-synthesised materials, whereas soaking in saline solutions

caused nearly complete amorphisation (Figures S8-9). ATR-IR displays a marked decrease in the intensity of the nitrate band at 1320 cm^{-1} for MIP-202-NO_3 upon treatment in HCl and NaCl (Figure S10). Conversely, in the case of MIP-202-Cl the nitrate band clearly appears after exposure to HNO_3 and $NaNO_3$ (Figure S11). Notably, the amount of MOF recovered was lower when the powders were soaked in saline solutions (57 and 68 mg for MIP-202-NO_3 and MIP-202-Cl, respectively, starting from 100 mg of each MOF) than in acidic solutions (75 and 80 mg for MIP-202-NO_3 and MIP-202-Cl, respectively, starting from 100 mg of each MOF), confirming the higher hydrolytic stability of the MOFs in acidic conditions. The chemical composition of the MOFs after treatment in acidic solutions was investigated by CHN and quantitative NMR spectroscopy (Figures S12-S15, Table S2). 70% of chloride was exchanged for nitrate in MIP-202-NO_3, yielding a MOF of formula $Zr_6O_4(OH)_4(C_4H_5NO_4)_6(HCl)_{4.2}(HNO_3)_{1.8}$. In the case of MIP-202-Cl, the composition after ion exchange was found to be $Zr_6O_4(OH)_4(C_4H_5NO_4)_6(HCl)_{1.8}(HNO_3)_{4.9}$, corresponding to 76% of the original chloride being replaced by nitrate.

The hydrolytic stability of MIP-202-NO_3 was further evaluated by dispersing 200 mg of MOF in either 200 or 20 mL of deionised water, refreshing the solvent every 2 h five times. The amount of nitrate released in solution was monitored using a UV-Vis based method (see experimental section in the ESI for details).[29,30] The pH of the solution was also monitored during each cycle. MIP-202-NO_3 released almost 60% of its nitrate content after the first cycle when 200 mg was dispersed in 200 mL of water, with a pH of the supernatant of about 2.8 (Figure 3, Figure S16). During the following cycles, the amount of nitrate released progressively decreased, while the pH of the supernatant increased up to about 4.0. The mass of solid recovered after the fifth cycle was 73 mg. Even considering losses due to incomplete recovery of the solid by centrifugation after each cycle, such a mass loss appears to suggest significant dissolution of MIP-202-NO_3. Inductively couple plasma optical emission spectroscopy (ICP-OES) analysis of the supernatant revealed that some Zr had in fact leached in solution, even though in amounts not compatible with the large drop observed in the mass of the solid (Table S3). To follow the fate of the aspartate, we suspended 2 mg of MIP-202-NO_3 in 2 mL of D_2O for one hour and performed ^{1}H-NMR analysis on the supernatant. The spectrum displayed no evidence of the presence of aspartate (Figure S17). Quantitative ^{1}H-NMR analysis of the solid recovered after five washing cycles in water and digested in alkaline medium, reveals that the aspartate content is 45.4 wt% (Figure S18). A C/N molar ratio > 4 is obtained by CHN analysis, suggesting complete leaching of nitrate from the solid (Asp has a C/N molar ratio of 4) (Table S4). The amount of aspartate obtained by NMR is compatible with the formula $Zr_6O_4(OH)_4(Asp)_{4.8}(OH/H_2O)_{2.4}$, where 20% of the original aspartate was lost over the five cycles, replaced by hydroxide/water couples. The PXRD pattern of the MOF after the fifth cycle displays a loss of long-range order and a shift of the reflections to higher 2θ values (Figure S19), which is accompanied by the disappearance of the nitrate stretching band in the ATR-IR spectrum (Figure S20). When 200 mg of MIP-202-NO_3 was dispersed in 20 mL of water, the amount of nitrate released in solution was less than 20% of the original content after the first cycle, with a pH of the supernatant of about 2.1 (Figure S21). After the fifth cycle, the amount of nitrate released was in the range of 5%, with a pH value of about 2.8. Similar experiments carried out using ethanol in place of water revealed a much lower leaching of nitrate in the less polar solvent (Figure 3).

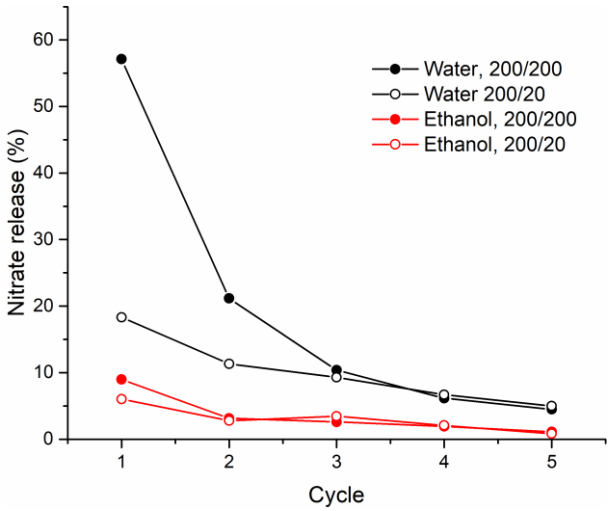

Figure 3. Release of nitrate from 200 mg of MIP-202-NO_3 over repeated cycles of soaking for 2 h in 200 mL of water (filled black circles), 20 mL of water (empty black circles, 200 mL of ethanol (filled red symbols) and 20 mL of ethanol (empty red circles).

These results suggest that MIP-202-NO_3 is unstable towards hydrolysis when dispersed in water and the release of nitrate appears to be accompanied by the release of protons. Suspending 20 mg of UiO-66 (both defect-free and defective, with formic acid as defect-compensating species) and MOF-801 in in 20 mL of water, we measured pH values of 4.5, 4.2 and 4.1, respectively. All these Zr-based MOFs contain the $[Zr_6O_4(OH)_4]^{12+}$ inorganic clusters and it was shown that the acidic reaction of UiO-66 in water is associated with leaching of monocarboxylic acids and not deprotonation of μ_3-OH groups.[31] In MIP-202-NO_3, the only source of protons, besides the μ_3-OH groups, can be the ammonium groups of the Asp linker. These groups display a pK_a of 9.66,[32] suggesting that they should stay protonated in water. Leaching of Asp from the solid upon hydrolysis of the linker-metal bonds could play a role, as the released Asp might have at least one of the carboxylic groups protonated (pK_a values of 1.95 and 3.71, respectively).[27] However, such leaching is substoichiometric with respect to the observed amount of nitrate released, leading us to conclude that most nitrate is released in the form of HNO_3 upon deprotonation of the ammonium groups of the linker, whose acidity might be enhanced upon coordination of the carboxylate groups to Zr. Soil has a typical pH between 3 and 10, depending on the location, and about one-third of the world's soil is calcareous, *i.e.*, alkaline.[33] Given that crushed sulfur and ammonium fertilisers are commonly used as acidifiers for alkaline soils, MIP-202-NO_3 could be used in analogous conditions.

Next, the release of nitrate in diluted saline solutions was monitored (Figure 4). About 80% of the nitrate was released in 1 h in 0.01 M NaCl, while at NaCl concentration of 0.001 M the release reached about 70% after 2 h. Higher concentrations of NaCl were not tested because chloride can interfere with the nitrate quantification method employed here.[29] Treatment of MIP-202-NO_3 with 0.01 and 0.001 M solutions of Na_2SO_4 resulted in very rapid exchange: at least 90% of nitrate release occurred in 1 h at both 0.01 M and 0.001 M sulfate concentration. In all cases, the nitrate release was higher than the baseline in water, suggesting that ion exchange took place to some extent, besides deprotonation of the MOF. The fact that sulfate triggered a larger release of nitrate can be attributed to the sulfate/nitrate exchange ratio being 1:2, whereas in the case of chloride the ratio is 1:1. This makes the exchange process more entropically favourable in the case of sulfate. In general, most of the nitrate release occurred as soon as the MOF was contacted with the solutions. This behaviour is comparable to what observed for (acrylamide-co-itaconic acid) hydrogels loaded with KNO_3,[8] while ethylcellulose-coated ammonium nitrate granules and LDHs display a slower release rate, in some cases exceeding 48 hours for the complete release.[6,7,10]

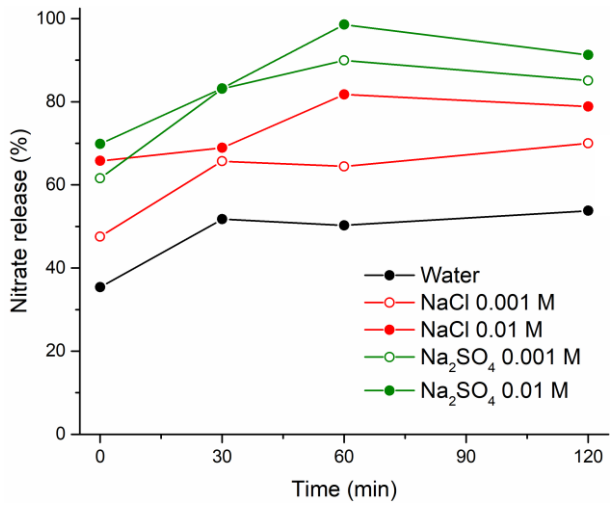

Figure 4. Release of nitrate from 200 mg of MIP-202-NO_3 dispersed in water (black circles), NaCl 0.001 M (red empty circles), NaCl 0.01 M (red filled circles), Na_2SO_4 0.001 M (green empty circles) and Na_2SO_4 0.01 M (green filled circles).

Conclusions

We successfully carried out the synthesis of MIP-202-NO_3 in aqueous medium starting from *L*-aspartic acid and zirconium oxynitrate in the presence of HNO_3. This MOF features a cationic framework, with nitrate anions residing in the pores. MIP-202-NO_3 is isostructural with the previously reported MIP-202-Cl and the two MOFs can be interconverted into each other by anion exchange in acidic solutions preserving their crystallinity. MIP-202-NO_3 contains 20.3 wt% of nitrate and displays limited hydrolytic stability, associated with fast release in solution of nitrate and protons. When dispersed in diluted solutions of chloride and sulfate, MIP-202-NO_3 releases between 70 and 90% of its nitrate loading within 2 h. To the best of our knowledge, this work is the first report of a MOF evaluated for its nitrate release properties. While the rate of nitrate release from a free-flowing powder of MIP-202-NO_3 is higher than that of other controlled release systems reported in the literature, the identification of a suitable formulation for this MOF, such as, *e.g.*, preparation of pellets in the presence of a biodegradable binder to slow down the release, could make it a potential candidate as a platform for controlled release of nitrate.

Author Contributions

T.O.A.: Conceptualization, Formal Analysis, Investigation, Writing – original draft, Writing – review & editing; M.K. and J.D.: Investigation, Writing – review & editing; M.T.: Conceptualization, Formal Analysis, Investigation, Supervision, Writing – original draft, Writing – review & editing; Resources.

Acknowledgment

The authors thank Diletta Morelli Venturi (University of Perugia) for performing PXRD analysis. Prof. Riccardo Vivani and Prof. Ferdinando Costantino (University of Perugia) are acknowledged for providing access to the diffractometer. Dr. Sandro Francesconi (University of Pisa) is acknowledged for the support provided during ICP-OES analysis. Dr. Randa Ishak (University of Pisa) is acknowledged for the support provided during SEM analysis. Centro per l'Integrazione della Strumentazione Scientifica dell'Università di Pisa (CISUP) is acknowledged for the use of the FEI Quanta 450 ESEM FEG. T.O.A. thanks the University of Pisa for funding *via* the Visiting Fellows programme.

Conflicts of interest

There are no conflicts to declare.

Notes and references

1 M. Calabi-Floody, J. Medina, C. Rumpel, L. M. Condron, M. Hernandez, M. Dumont and M. de la L. Mora, *Smart Fertilizers as a Strategy for Sustainable Agriculture*, Elsevier Inc., 1st edn., 2018, vol. 147.

2 S. Singh, A. G. Anil, V. Kumar, D. Kapoor, S. Subramanian, J. Singh and P. C. Ramamurthy, *Chemosphere*, 2022, **287**, 131996.

3 K. c. Cameron, H. j. Di and J. l. Moir, *Annals of Applied Biology*, 2013, **162**, 145–173.

4 C. J. Ransom, V. D. Jolley, T. A. Blair, L. E. Sutton and B. G. Hopkins, *PLOS ONE*, 2020, **15**, e0234544.

5 G. L. Velthof, P. J. Kuikman and O. Oenema, *Biol Fertil Soils*, 2003, **37**, 221–230.

6 S. Pérez-García, M. Fernández-Pérez, M. Villafranca-Sánchez, E. González-Pradas and F. Flores-Céspedes, *Ind. Eng. Chem. Res.*, 2007, **46**, 3304–3311.

7 M. D. Ureña-Amate, N. D. Boutarbouch, M. del M. Socias-Viciana and E. González-Pradas, *Applied Clay Science*, 2011, **52**, 368–373.

8 M. M. Urbano-Juan, M. M. Socías-Viciana and M. D. Ureña-Amate, *Reactive and Functional Polymers*, 2019, **141**, 82–90.
9 M. R. Berber and I. H. Hafez, *Bull Environ Contam Toxicol*, 2018, **101**, 751–757.
10 A. M. Kotlar, H. Wallace Pereira de Carvalho, B. V. Iversen and Q. de Jong van Lier, *Applied Clay Science*, 2020, **184**, 105365.
11 A. Singha Roy, S. Kesavan Pillai and S. S. Ray, *ACS Omega*, 2023, **8**, 8427–8440.
12 D.-W. Sun, L. Huang, H. Pu and J. Ma, *Chem. Soc. Rev.*, 2021, **50**, 1070–1110.
13 S. Rojas, A. Rodríguez-Diéguez and P. Horcajada, *ACS Appl. Mater. Interfaces*, 2022, **14**, 16983–17007.
14 L. A. M. Mahmoud, R. A. dos Reis, X. Chen, V. P. Ting and S. Nayak, *ACS Omega*, 2022, **7**, 45910–45934.
15 J. Yang, C. A. Trickett, S. B. Alahmadi, A. S. Alshammari and O. M. Yaghi, *J. Am. Chem. Soc.*, 2017, **139**, 8118–8121.
16 Y. Shan, L. Cao, B. Muhammad, B. Xu, P. Zhao, C. Cao and Q. Huang, *Journal of Colloid and Interface Science*, 2020, **566**, 383–393.
17 M. Anstoetz, T. J. Rose, M. W. Clark, L. H. Yee, C. A. Raymond and T. Vancov, *PLOS ONE*, 2015, **10**, e0144169.
18 K. Wu, X. Xu, F. Ma and C. Du, *ACS Omega*, 2022, **7**, 35970–35980.
19 B. Sierra-Serrano, A. García-García, T. Hidalgo, D. Ruiz-Camino, A. Rodríguez-Diéguez, G. Amariei, R. Rosal, P. Horcajada and S. Rojas, *ACS Appl. Mater. Interfaces*, 2022, **14**, 34955–34962.
20 B. K. Jung, Z. Hasan and S. H. Jhung, *Chemical Engineering Journal*, 2013, **234**, 99–105.
21 X. Zhu, B. Li, J. Yang, Y. Li, W. Zhao, J. Shi and J. Gu, *ACS Appl. Mater. Interfaces*, 2015, **7**, 223–231.
22 I. Akpinar, R. J. Drout, T. Islamoglu, S. Kato, J. Lyu and O. K. Farha, *ACS Appl. Mater. Interfaces*, 2019, **11**, 6097–6103.
23 R. J. Drout, L. Robison, Z. Chen, T. Islamoglu and O. K. Farha, *Trends in Chemistry*, 2019, **1**, 304–317.
24 I. Abánades Lázaro and R. S. Forgan, *Coordination Chemistry Reviews*, 2019, **380**, 230–259.
25 H. A. Schroeder and J. J. Balassa, *Journal of Chronic Diseases*, 1966, **19**, 573–586.
26 M. Shahid, E. Ferrand, E. Schreck and C. Dumat, in *Reviews of Environmental Contamination and Toxicology Volume 221*, ed. D. M. Whitacre, Springer New York, New York, NY, 2013, pp. 107–127.
27 S. Wang, M. Wahiduzzaman, L. Davis, A. Tissot, W. Shepard, J. Marrot, C. Martineau-Corcos, D. Hamdane, G. Maurin, S. Devautour-Vinot and C. Serre, *Nat Commun*, 2018, **9**, 4937.
28 G. Socrates, *Infrared and Raman Characteristic Group Frequencies: Tables and Charts*, 3rd Edition., 2004.
29 W. P. Robarge, A. Edwards and B. Johnson, *Communications in Soil Science and Plant Analysis*, 1983, **14**, 1207–1215.
30 D. A. Cataldo, M. H. Haroon, L. E. Schrader and V. L. Youngs, *Communications in Soil Science and Plant Analysis*, 1975, **6**, 71–80.
31 D. Bůžek, J. Demel and K. Lang, *Inorg. Chem.*, 2018, **57**, 14290–14297.
32 J. Rumble, *CRC Handbook of Chemistry and Physics*, CRC Press, Boca Raton, FL, 100th edn., 2019.
33 A. Wallace, *Communications in Soil Science and Plant Analysis*, 1994, **25**, 87–92.